

Unoccupied electronic structure of graphite probed by angle-resolved photoemission spectroscopy

S. K. Mahatha and Krishnakumar S. R. Menon*

Surface Physics Division, Saha Institute of Nuclear Physics, 1/AF Bidhannagar, Kolkata 700064, India

T. Balasubramanian

MAXLAB, Lund University, P.O. Box 118, S-221 00 Lund, Sweden

(Received 2 May 2011; revised manuscript received 28 July 2011; published 16 September 2011)

We report the observation of anomalous bands in graphite valence band structure in angle-resolved photoemission spectroscopy (ARPES) experiments. The photon energy dependence of these bands shows a constant kinetic energy nature. Our results are supported by the very low energy electron diffraction data reported on graphite surfaces which essentially map the unoccupied states representing the photoemission final states. This suggests that the ARPES technique is capable of probing the unoccupied electronic states governed by the secondary electron emission process, along with the occupied bands of solids.

DOI: [10.1103/PhysRevB.84.113106](https://doi.org/10.1103/PhysRevB.84.113106)

PACS number(s): 79.60.-i, 71.20.-b, 73.20.-r

The electronic band structure of graphite has been intensively studied both theoretically and experimentally as it is considered a prototypical two-dimensional material.¹⁻⁴ The interest in graphite has been renewed recently because of the discovery of graphene out of graphite by peeling off the top layer using scotch tape.⁵ Graphene has become one of the most promising material for future electronics due to its exceptional electronic structure around the Fermi energy.⁶ The valence band of graphite consists of $2s$, $2p_x$, $2p_y$ orbital derived σ bands and the $2p_z$ derived π band which crosses the Fermi energy, making graphite conductive. The conduction band consist of σ^* and π^* bands. In agreement with its two-dimensional layered crystal structure and strong anisotropic properties, the band structure calculations² show strong localization perpendicular to the basal planes while explaining most of the in-plane dispersions.

Angle-resolved photoemission spectroscopy (ARPES) is a widely used and powerful tool to determine the occupied valence band structure of crystalline solid surfaces with high energy and wave vector (\mathbf{k}) resolutions.⁷ Because of its high surface sensitivity, ARPES has difficulty in determining the perpendicular component of the wave vector (\mathbf{k}_\perp) as the periodicity breaks at the surface whereas the parallel component of the wave vector (\mathbf{k}_\parallel) conserves. Thus, ARPES contains information of the occupied band dispersions along \mathbf{k}_\parallel . It has been demonstrated by Strocov *et al.*^{8,9} that the unoccupied bands can be mapped by the very low energy electron diffraction (VLEED) experiment which relies on the fact that the photoemission final states are time-reversed LEED states in one-step model. The VLEED spectroscopy does not include the initial states unlike the other unoccupied-state spectroscopies, such as inverse photoemission spectroscopy (IPS). So, the final-state information provided by VLEED spectroscopy can be used to determine the occupied valence band structures along the \mathbf{k}_\perp direction and thus the complete three-dimensional band structure can be obtained.¹⁰

The ARPES data may contain VLEED information (i.e., the photoemission final states) if one collect the very low kinetic energy part of the photoemission spectrum, which is essentially populated by the secondary electrons.¹¹⁻¹³ These secondary electrons can interfere constructively with the

crystal potential and relax to some scattering states. If these scattering states get coupled with the vacuum, the electron can escape into the vacuum and subsequently be detected. Thus, secondary electron emission (SEE) intensity is governed by the transition of the cascade electrons from the higher energy (unoccupied) levels to the vacuum. Based on these facts, we may conclude that the angle-resolved secondary electron emission spectroscopy (ARSEES) can give detailed \mathbf{k} -resolved information of the unoccupied states.^{14,15}

In this Brief Report, we present the ARPES measurements on highly oriented pyrolytic graphite (HOPG) and single-crystal graphite samples up to the range of secondary electrons. In addition to the well-known valence band structures of graphite, we observe some anomalous bands which appear as constant kinetic energy features at different photon energies. These bands are neither reported earlier in ARPES of graphite nor predicted by the bulk band structure calculations.¹⁻³ Our experimental results are discussed with respect to the VLEED experiments performed by Strocov *et al.*²¹ which essentially probe the photoemission final states, showing that VLEED information can be obtained in the ARPES experiments. This makes ARPES a versatile experimental tool for mapping both the occupied and unoccupied part of band structure with high \mathbf{k} resolution.

The ARPES measurements were performed using a laboratory setup as well as using a synchrotron source (beamline I4 of the MAX synchrotron radiation laboratory, Sweden). The laboratory ARPES experiments were performed using a combination of the SCIENTA-R4000WAL electron energy analyzer with a 2D-CCD detector and a high-flux GAMMA-DATA VUV He lamp attached with a VUV monochromator; the details have been outlined elsewhere.¹⁶ During experiments the base pressure of the measurement chamber was kept below 4×10^{-11} mbar. We used He I α (21.218 eV) and He II α (40.814 eV) resonance lines to excite the photoelectrons from the sample surface. The HOPG crystals were cleaved *in situ* using scotch tape while the graphite single crystals of large sizes (4–5 mm diameter) (Nanotech Innovations, USA) were cleaved *in situ* using an aluminum post in the preparation chamber in an ultrahigh vacuum better than 5×10^{-10} mbar. For synchrotron experiments, the experimental chamber was

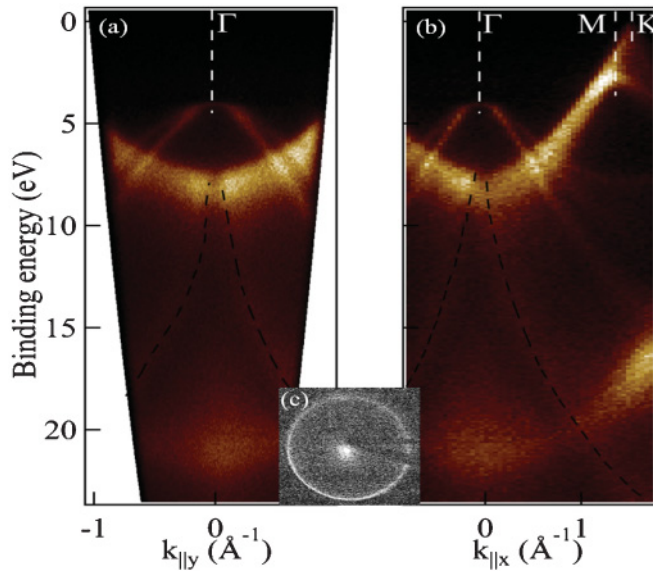


FIG. 1. (Color online) (a) ARPES spectra of HOPG measured at room temperature using He II α resonance line along $\mathbf{k}_{\parallel y}$ and (b) $\mathbf{k}_{\parallel x}$ symmetry directions. (c) LEED image of HOPG using 70 eV electrons. The black dashed lines are guides to the eye showing the weak anomalous bands.

equipped with a SPECS PHIBOS-100 analyzer with 2D-CCD detector. The undulator beamline provided high-intensity linear polarized photons from 15 eV to about 160 eV which were used for the photon energy dependent ARPES measurements. All the experiments were performed at room temperature with an angular resolution better than 0.8° .

Figures 1(a) and 1(b) show the valence band ARPES spectra along the $\mathbf{k}_{\parallel y}$ and $\mathbf{k}_{\parallel x}$ directions of the HOPG crystal using the He II α resonance line with the laboratory setup.¹⁷ We observe the σ and π bands at the same energy position and with consistent dispersions with the previous ARPES measurements.^{1,3} However, along with these familiar graphite valence bands, we also observe another set of weak dispersive anomalous bands [see in Figs. 1(a) and 1(b) as black dashed lines] which are not predicted by the bulk band structure calculations.² These bands are symmetric in nature along both $\mathbf{k}_{\parallel x}$ and $\mathbf{k}_{\parallel y}$ directions suggesting that these are intrinsically related to the HOPG band structure. However, these anomalous bands could not be observed in the ARPES spectrum using the He I α resonance line (not shown). It should be noted that HOPG is a quasi-single crystal, with perfect ordering along the (0001) direction but with an intrinsic rotational disorder of the individual microcrystals within the plane of the crystal. This azimuthal disorder in HOPG is manifested by the circular LEED rings as shown in Fig. 1(c). This raises a question on the presence of the observed anomalous bands in Fig. 1. Is it an intrinsic nature of graphite or that of HOPG crystals?

To address this issue, we have performed ARPES experiments on high-quality single crystals of graphite in the laboratory as well as using the synchrotron facility. Figures 2(a) and 2(b) show the ARPES spectra obtained from graphite single crystals using 41 eV photons (synchrotron experiments) along the ΓM and ΓK symmetry directions, respectively. The sharp hexagonal LEED spots at 70 eV confirm the surface

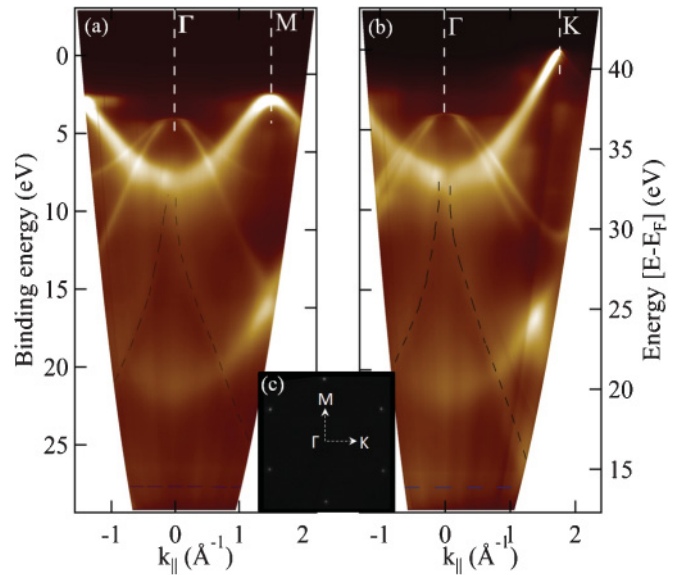


FIG. 2. (Color online) ARPES spectra of single-crystal graphite using 41 eV photons along (a) ΓM and (b) ΓK symmetry direction. (c) LEED pattern of single-crystal graphite at 70 eV with symmetry directions shown. The blue dashed line around 14 eV in $[E - E_F]$ energy scale corresponds to SEE feature.

single-crystalline nature (without any twins), cleanliness and the symmetry directions as shown in Fig. 2(c). The same dispersing anomalous bands can be observed in Figs. 2(a) and 2(b) with similar dispersions along both the ΓM and ΓK directions. Our laboratory experiments on single-crystal graphite surfaces also shows the existence of these features confirming that the observed anomalous bands are the intrinsic nature of the graphitic system.

In order to study the origin of these anomalous bands, we have performed ARPES measurements at different photon energies using the synchrotron source. The same anomalous bands can be observed in the ARPES spectra shown in Fig. 3, for different photon energies (47, 53, and 70 eV are shown for example). Apart from the anomalous bands observed at 41 eV ARPES spectra (see Figs. 1 and 2), we can see more anomalous features visible at 70 eV photon energy. There is a nondispersing band near 33 eV and an upper dispersing band ranging from 34.5 eV to about 44.5 eV in $[E - E_F]$ scale, marked by black dashed lines. These weak anomalous bands were not visible or partly visible in lower photon energies as those were masked by the valence bands of the graphite. At 70 eV photon energy, the anomalous bands are in a region free of valence band structures of graphite, and can be distinguished rather clearly. The energy positions of all these anomalous bands show a constant kinetic energy (constant energy in $[E - E_F]$ scale) nature for different photon energies as shown in Fig. 3. It is also clear from Figs. 3(c) and 3(d) that there is no change in dispersion along the ΓK and ΓM symmetry direction up to 0.8 \AA^{-1} in \mathbf{k} as observed in Figs. 1 and 2. In Fig. 3(e), the ARPES spectra at 70 eV photon energy along the ΓK direction is shown in a waterfall graph and the anomalous dispersing bands have been marked by dashed lines.

Along with these anomalous bands, we observe two more near-flat bands in the low-energy regions. At about 19.5 eV

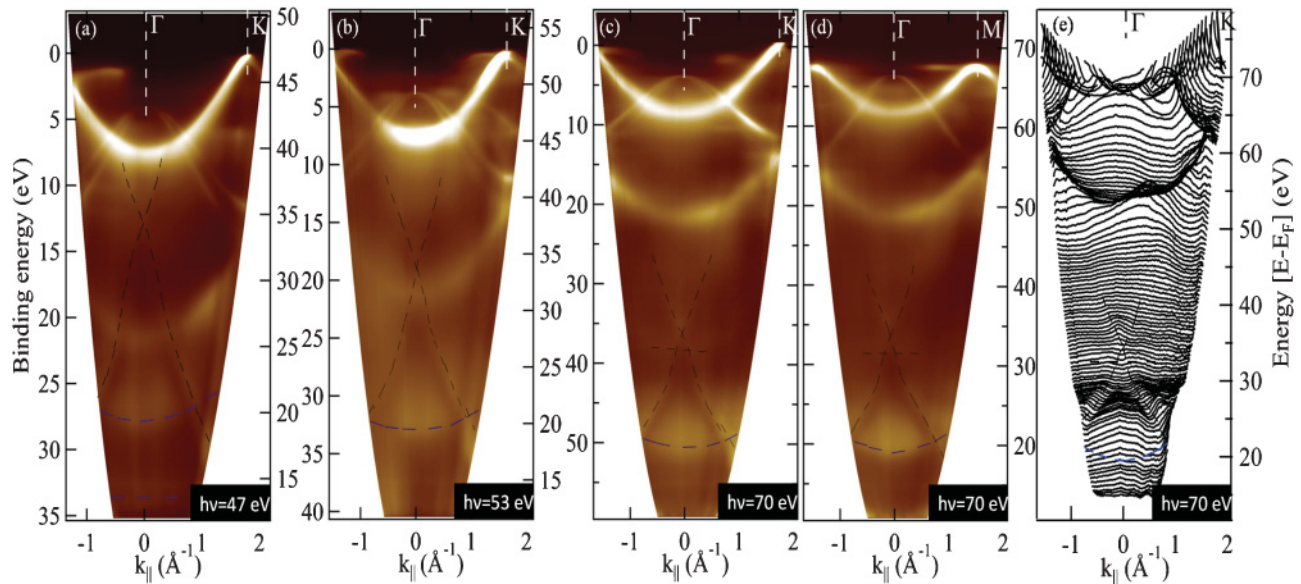


FIG. 3. (Color online) ARPES spectra of graphite single crystal using (a) 47 eV photon energy along ΓK symmetry direction, (b) 53 eV photon energy along ΓK direction, (c) 70 eV photon energy along ΓK direction, (d) 70 eV photon energy along ΓM direction. The ARPES spectra for 70 eV photon energy along ΓK direction is shown as waterfall graph in (e). Anomalous bands are shown with black dashed lines. The blue dashed lines show the (σ^*) features due to the SEE process.

energy, we observe a weakly dispersive band as shown (by blue dashed line) in Fig. 3. This band is known to originate from the (σ^*) conduction band in graphite with Γ_4^- symmetry due to the SEE as shown by earlier studies.⁴ We also observe a faint flat band near 14 eV energy in 41 eV and 47 eV ARPES spectra as shown in Figs. 2 and 3(a), respectively. This SEE feature is also known^{2,4} to arise from the (σ^*) conduction bands of Γ_1^+ and Γ_4^- symmetry with the minima at 14 eV above the Fermi level (9.5 eV kinetic energy with a work function of 4.5 eV). However, this band is not visible for higher photon energies, possibly due to cross-section effects. The strongest (σ^*) band with Γ_1^+ symmetry (interlayer band) appears as a SEE feature at 3 eV kinetic energy.^{18–20} However, we could not observe this feature as we did not probe such low kinetic energies.

From the observation of the constant energy nature of these anomalous bands at different photon energies (black dashed lines in Fig. 4), we propose that these bands are originated from the unoccupied states or photoelectron final-state bands of graphite due to the SEE process. The photoelectrons excited from the valence bands undergo a series of inelastic scattering and produce cascaded secondary electrons. These secondary electrons make transitions to the high-lying conduction bands or unoccupied bands from which they escape into the vacuum without any memory of the initial occupied states of the photoelectrons.¹⁵ Since the VLEED experiment maps the unoccupied valence band structures in the solid, we compare our ARPES experimental results with the reported VLEED data on graphite single crystals by Strocov *et al.*²¹ In Fig. 4, we show the anomalous band dispersions on a graphite single crystal obtained from our ARPES experiments in Fig. 3 (shown by black circles) along with the dispersions reported using VLEED experiments²¹ (red triangles). Here, the energy scale adopted is that of the secondary electrons, i.e., from the Fermi level of the sample. The energy position and the dispersions of the upper dispersing constant energy band (from

34.5 eV to 44.5 eV above E_F) and the nondispersing band at around 33 eV above E_F are in quite good agreement with the unoccupied bands obtained from the VLEED experiment, whereas there seems to be a mismatch in the dispersion of the lower dispersing bands (from 34.5 to 18.5 above E_F) which could be due the experimental uncertainty in the determination of the bands in this region. The band positions were determined from the intensity variations as observed from the ARPES images in Figs. 1, 2, and 3. However, the determination of their exact positions by fitting procedures were difficult due to the fine-structured background. Still, we can observe a near one-to-one correspondence of the SEE features in the ARPES spectra and the VLEED data of single-crystal graphite

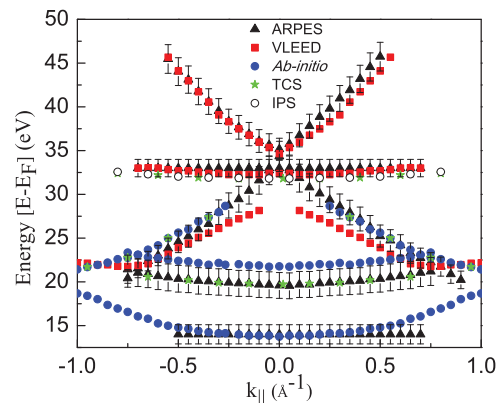


FIG. 4. (Color online) Comparison of the energy position and dispersion of SEE features observed in the ARPES spectra with the VLEED results reported by Strocov *et al.* (Ref. 21) on graphite single crystals. Results from the target current spectroscopy (TCS) (Ref. 18) and IPS (Ref. 19) experiments and *ab initio* calculations of Tatar and Rabbii (Ref. 2) are also compared. The width of the measured SEE features in ARPES spectra are shown as error bars.

samples. The constant 19.5 eV energy (σ^*) band of Γ_4^- symmetry and 14 eV constant energy feature of Γ_1^+ and Γ_4^- symmetry in the ARPES spectra could not be associated with the experimental VLEED data.²¹

From a comparison with the *ab initio* band structure calculations by Tatar and Rabi² and from the TCS experiments,¹⁸ the lower dispersing bands seem to be originating from the π^* conduction band in graphite. The energy positions as well as the dispersions of the lower dispersing bands are in similitude with the TCS data and calculated π^* conduction band of Γ_2^- symmetry whose energy maximum is beyond the energy range of band structure calculations² (see Fig. 4). Also, the nondispersing band near 33 eV above E_F matches well with the TCS¹⁸ and IPS data,¹⁹ as shown in Fig. 4. As there are no calculated or TCS data available above 34.5 eV above E_F , at present we are unable to conclude on the character of the upper dispersing bands. The σ^* band at 19.5 eV matches well with the TCS data whereas there is a small mismatch with the *ab initio* calculation. However, the nondispersing σ^* band at 14 eV energy matches well with the *ab initio* band structure calculations by Tatar and Rabi.² From the photon energy dependence of the lower and upper dispersing bands at normal emission (Γ) (not shown), the band energy positions

show a weak dispersion of about 1 eV. This is similar to the observation of the \mathbf{k}_\perp dispersion observed for the π bands at normal emission.⁴

In conclusion, we report the presence of the unoccupied bands or photoelectron final states in the ARPES spectra of HOPG and single-crystal graphite systems. The unoccupied bands were mapped by the SEE process which was produced by the cascaded scattering process of the photoelectron ejecting from the valence band. We show the equivalence of the VLEED and ARSEES processes of mapping the unoccupied bands of graphite, in agreement with earlier studies. In particular, the experimental ARPES spectra on graphite supports the idea of mapping the unoccupied bands or photoelectron final states by performing ARPES up to the low kinetic energy (secondary electron energy) region.

A part of this work was carried out at the MAX synchrotron radiation facility, Sweden, with the financial support of Department of Science and Technology, Government of India, through the S. N. Bose National Centre for Basic Science, India. We acknowledge the Micro-Nano initiative programme of the Department of Atomic Energy (DAE), Government of India, for generous funding and support.

*Corresponding author: krishna.menon@saha.ac.in

¹S. Y. Zhou, G.-H. Gweon, C. D. Spataru, J. Graf, D.-H. Lee, Steven G. Louie, and A. Lanzara, *Phys. Rev. B* **71**, 161403 (2005).

²R. C. Tatar and S. Rabi, *Phys. Rev. B* **25**, 4126 (1982).

³S. Y. Zhou, G.-H. Gweon, and A. Lanzara, *Ann. Phys. (N.Y.)* **321**, 1730 (2006).

⁴A. R. Law, M. T. Johnson, and H. P. Hughes, *Phys. Rev. B* **34**, 4289 (1986).

⁵K. S. Novoselov, A. K. Geim, S. V. Morosov, D. Jiang, Y. Zhang, S. V. Dubonos, I. V. Grigorieva, and A. A. Firsov, *Science* **306**, 666 (2004).

⁶A. H. Castro Neto, F. Guinea, N. M. R. Peres, K. S. Novoselov, and A. K. Geim, *Rev. Mod. Phys.* **81**, 109 (2009).

⁷S. Hüfner, *Photoelectron Spectroscopy* (Springer, Berlin, 1995).

⁸E. E. Krasovskii, W. Schattke, V. N. Strocov, and R. Claessen, *Phys. Rev. B* **66**, 235403 (2002).

⁹V. N. Strocov, H. I. Starnberg, and P. O. Nilsson, *J. Phys. Condens. Matter* **8**, 7539 (1996).

¹⁰V. N. Strocov, R. Claessen, G. Nicolay, S. Hüfner, A. Kimura, A. Harasawa, S. Shin, A. Kakizaki, H. I. Starnberg, P. O. Nilsson, and P. Blaha, *Phys. Rev. B* **63**, 205108 (2001).

¹¹M. Bovet, V. N. Strocov, F. Clerc, C. Koitzsch, D. Naumovic, and P. Aebi, *Phys. Rev. Lett.* **93**, 107601 (2004).

¹²V. N. Strocov, H. I. Starnberg, P. O. Nilsson, H. E. Brauer, and L. J. Holleboom, *Phys. Rev. Lett.* **79**, 467 (1997).

¹³V. N. Strocov, R. Claessen, G. Nicolay, S. Hüfner, A. Kimura, A. Harasawa, S. Shin, A. Kakizaki, P. O. Nilsson, H. I. Starnberg, and P. Blaha, *Phys. Rev. Lett.* **81**, 4943 (1998).

¹⁴F. Maeda, T. Takahashi, H. Ohsawa, S. Suzuki, and H. Suematsu, *Phys. Rev. B* **37**, 4482 (1988).

¹⁵L. S. Caputi, G. Chiarello, A. Santaniello, E. Colavita, and L. Papagno, *Phys. Rev. B* **34**, 6080 (1986).

¹⁶S. K. Mahatha and Krishnakumar S. R. Menon, *Curr. Sci.* **98**, 759 (2010).

¹⁷ $\mathbf{k}_{\parallel x}$ and $\mathbf{k}_{\parallel y}$ are defined as the momentum dispersions along the orthogonal directions of the analyzer (Ref. 16).

¹⁸R. Claessen, H. Carstensen, and M. Skibowski, *Phys. Rev. B* **38**, 12582 (1988).

¹⁹I. Schäfer, M. Schlüter, and M. Skibowski, *Phys. Rev. B* **35**, 7663 (1987).

²⁰M. Breitholtz, J. Algdal, T. Kihlgren, S.-Å. Lindgren, and L. Walldén, *Phys. Rev. B* **70**, 125108 (2004).

²¹V. N. Strocov, P. Blaha, H. I. Starnberg, M. Rohlfling, R. Claessen, J.-M. Debever, and J.-M. Themlin, *Phys. Rev. B* **61**, 4994 (2000).